Bounding of effective thermal conductivities of multiscale materials by essential and natural boundary conditions

M. Ostoja-Starzewski
Institute of Paper Science and Technology, 500 10th Street, Atlanta, Georgia 30318-5794

J. Schulte
Department of Applied Physics, University of Technology, Sydney, P.O. Box 123, Broadway, NSW 2007, Australia
(Received 8 May 1995; revised manuscript received 30 October 1995)

We demonstrate the bounding of the effective properties of random multiscale microstructures by means of essential and natural boundary conditions. The proposed method involves moderate sized lattices, not modified in the boundary zone, thereby allowing much faster calculations than the method of periodic boundary conditions. In case of a random two-phase lattice, scaling laws have been found for a wide range of contrasts. In the case of a disk-inclusion composite having circular inclusions with graded interphases, the presence of a graded interphase dramatically changes the effective conductivity compared to that of a composite with perfect interfaces. [S0163-1829(96)01122-8]

I. INTRODUCTION

The past decade has seen a great activity in physics of heterogeneous systems. More specifically, much attention has been focused on problems involving conductivity and elasticity of two- and multiphase materials. While various rigorous analytical results and effective-medium theories have been developed for simple (periodic) microstructures,[1–4] computer simulations proved to be a valuable complement to the theoretical studies of composites in case of more materials. One example of the latter is a functionally graded material (FGM), that is, a material having a graded multiscale microstructure.

In this paper we adapt a method of two scale-dependent bounds to problems in thermal conductivity, and demonstrate its power and advantages on random media problems. In Sec. II, following an approach being developed in mechanics of heterogeneous solids,[5,6] we show that the effective conductivity on infinite length scales can be bounded with the help of the essential (Dirichlet) and natural (Neumann) boundary conditions. This methodology is illustrated in Sec. III in the context of two two-dimensional (2D) problems: (i) a two-phase random chessboard at 50% volume fraction for a range of contrasts from 1 through 10^4, and (ii) a composite material with perfect circular inclusions. Finite-size scaling is analyzed extensively in the first case.

Section IV discusses the main problem of this paper: thermal conductivity of a matrix-inclusion composite of circular inclusions (disks) with functionally graded interfaces, e.g., Refs. 7–10. In accordance with the method of two scale-dependent bounds, results of numerical calculations on the effective conductivities are presented for a range of contrasts from 1 through 10^4 at various matrix-inclusion volume fractions, where the contrast is defined as the ratio of conductivity of the inclusion phase to the matrix phase. We find that the presence of a rather narrow graded matrix-inclusion interphase dramatically changes the effective conductivity as compared to the one of a composite with perfect inclusions. Scaling laws dependent on the contrast are also derived. Finally, in Sec. V, we develop an effective-medium theory for functionally graded composites, which performs well at low contrasts. Conclusions and recommendations for further work are summarized in Sec. VI.

II. BOUNDING OF EFFECTIVE PROPERTIES BY ESSENTIAL AND NATURAL BOUNDARY CONDITIONS

Let us consider a *random microstructure* (or *random medium*) to be a family $\boldsymbol{B}=\{\boldsymbol{B}(\omega);\omega\in\Omega\}$ of deterministic media $\boldsymbol{B}(\omega)$, where ω is an indicator of a given realization, and Ω is an underlying sample space. Next, we introduce a so-called *window* $B_\delta(\omega)$ of scale

$$\delta=\frac{L}{d}, \tag{1}$$

where L is the window (or sample) size and d is the size of a heterogeneity, Fig. 1. The material is a matrix-inclusion composite with thermal conductivity of phases being $C^{(m)}$ and $C^{(d)}$ in the matrix (m) and the disk-inclusion (d) phases, respectively. This microstructure is assumed to have spatially homogeneous statistics (invariant with respect to translations) and to be ergodic (volume averages equal ensemble averages).

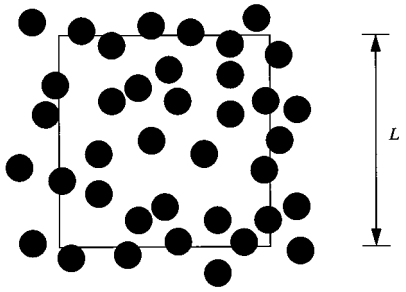

FIG. 1. A window of size L placed onto a matrix-inclusion composite having inclusions (round disks) of diameter d.

In order to define effective properties we have to consider δ values larger than 1, and two types of boundary conditions: (a) essential (Dirichlet, ''temperature-controlled'')

$$T=\overline{\nabla T}\cdot\vec{x}, \tag{2}$$

which yield a tensor $\mathbf{C}_\delta^e$ (e stands for essential boundary conditions), where T is the temperature, $\overline{\nabla T}$ is the spatial average temperature gradient, and $\vec{x}$ is a position vector, and (b) natural (Neumann, ''flux-controlled''):

$$\overline{\vec{q}}\cdot\vec{n}=\vec{q}\cdot\vec{n}, \tag{3}$$

which yield the tensor $\mathbf{C}_\delta^n=(\mathbf{S}_\delta^n)^{-1}$ (n stands for natural boundary conditions), where $\vec{q}$ is the heat flux, $\overline{\vec{q}}$ is the spatial average heat flux, and $\vec{n}$ is the outer unit normal to the window's boundary. In the above we employ boldface for a second-rank tensor, and an overbar for a spatial average over the window domain. Note that $\delta\to\infty$ is the conventional continuum limit typically sought in the effective-medium theories, while numerical simulations correspond to some finite δ.

We observe that $\mathbf{C}_\delta^e$ is, in general, different from $\mathbf{C}_\delta^n$ as it provides an *upper estimate* on the effective thermal conductivity of the given specimen, while the latter represents a *lower estimate*. In fact, it can be shown[5,6,11] (see also the Appendix) from the variational principles, that the effective macroscopic conductivity tensor $\mathbf{C}^{\text{eff}}$ is bounded by two tensors $\langle\mathbf{C}_\delta^e\rangle$ and $\langle\mathbf{S}_\delta^n\rangle^{-1}$, where $\langle\ \rangle$ denotes the ensemble averaging, i.e., averaging over the space of all realizations Ω. In elasticity problems one uses the principles of minimum potential energy and complementary energy. Both ensemble averages bound the effective conductivity the more the scale δ approaches its continuum limit $\delta\to\infty$. Thus, a hierarchy of δ-dependent bounds on $\mathbf{C}^{\text{eff}}$ can be derived

$$\mathbf{C}^R\equiv(\mathbf{S}^R)^{-1}\equiv\langle\mathbf{S}_1^n\rangle^{-1}\leqslant\langle\mathbf{S}_{\delta'}^n\rangle^{-1}\leqslant\langle\mathbf{S}_\delta^n\rangle^{-1}\leqslant\mathbf{C}^{\text{eff}}$$

$$\leqslant\langle\mathbf{C}_\delta^e\rangle\leqslant\langle\mathbf{C}_{\delta'}^e\rangle\leqslant\langle\mathbf{C}_1^e\rangle\equiv\mathbf{C}^V,\quad\forall\,\delta'<\delta. \tag{4}$$

In (4) $\mathbf{C}^V$ and $\mathbf{C}^R$ denote the (elementary) Voigt and Reuss bounds,[1] corresponding to windows at the smallest scale ($\delta=1$). In other words, the effective response depends on the boundary conditions, and the influence of the latter disappears as the sample becomes infinite. The order relation employed in (4) is to be understood as follows: for two second-rank tensors $\mathbf{A}$ and $\mathbf{B}$, the order relation $\mathbf{B}\leqslant\mathbf{A}$ means $\vec{t}\cdot\mathbf{B}\cdot\vec{t}\leqslant\vec{t}\cdot\mathbf{A}\cdot\vec{t}$ for any vector $\vec{t}\neq\vec{0}$. In the special case of the microstructure being characterized by isotropic statistics, $\mathbf{C}^{\text{eff}}$ is isotropic, i.e., $\mathbf{C}^{\text{eff}}=\mathbf{I}\mathbf{C}^{\text{eff}}$ where $\mathbf{I}$ is the identity tensor.

Another method of calculating effective properties typically used in solid-state physics, is based on the concept of a periodic window (with a heterogeneous microstructure of periodicity L or, equivalently, δ), i.e., periodic boundary conditions

$$T(\vec{x})=T(\vec{x}+\vec{L})+\overline{\nabla T}\cdot\vec{L},\quad\forall\vec{x}\in\partial\mathbf{B}, \tag{5}$$

$$\vec{q}(\vec{x})=-\vec{q}(\vec{x}+\vec{L}),\quad\forall\vec{x}\in\partial\mathbf{B}.$$

Here $\vec{L}=L\vec{e}$, where $\vec{e}$ is the unit vector. The effective conductivity obtained under such boundary conditions is denoted by $\mathbf{C}_\delta^{\text{per}}$. The ensemble average of this tensor, just as $\langle\mathbf{C}_\delta^e\rangle$ and $\langle\mathbf{S}_\delta^n\rangle^{-1}$, is isotropic for a microstructure of space-homogeneous and isotropic statistics. However, the method based on periodic boundary conditions has some major drawbacks compared to the one based on bounding the effective conductivity by essential and natural boundary conditions: (i) It modifies the actual microstructure to ensure its geometric periodicity; (ii) it yields only one estimate on $\mathbf{C}^{\text{eff}}$, i.e., $\langle\mathbf{C}_\delta^{\text{per}}\rangle$, and thus, in order to compensate for the scale (i.e., δ) dependence, it requires much larger lattices than those employed by the method proposed here; (iii) in cases of material instabilities (such as fracture propagation, or shear band formation) it restricts the range of possible response modes to the spatially periodic ones only.

A calculation involving both types of boundary conditions avoids unnaturally modifying the material (as it needs to be done using the periodic boundary conditions), while at the same time providing two rigorous bounds on $\mathbf{C}^{\text{eff}}$ for whatever δ. The choice of δ corresponds directly to the amount of computational effort involved, so that, the more extensive the computational time and effort, the closer are the bounds on $\mathbf{C}^{\text{eff}}$. It will be illustrated in the next section, however, that the method based on bounding by essential and natural boundary conditions already results in very close bounds at relatively small windows.

In order to solve the field equations of a two-phase composite we employ a finite difference scheme. The idea is to approximate the planar continuum by a very fine mesh. In the following, we shall assume that a square mesh for discretization of the temperature field T is used. The governing equations are thus

$$T(i,j)[k_r+k_l+k_u+k_d]-T(i+l,j)k_r-T(i-l,j)k_l$$
$$-T(i,j+l)k_u-T(i,j-l)k_d=0. \tag{6}$$

Here i and j are the coordinates of mesh points, and k_r, k_l, k_u and k_d are defined from the series spring model

$$\begin{aligned}k_r&=[1/C(i,j)+1/C(i+l,j)]^{-1},\\ k_l&=[1/C(i,j)+1/C(i-l,j)]^{-1},\\ k_u&=[1/C(i,j)+1/C(i,j+l)]^{-1},\\ k_d&=[1/C(i,j)+1/C(i,j-l)]^{-1},\end{aligned} \tag{7}$$

where $C(i,j)$ is the property at a point i,j.

III. A RANDOM TWO-PHASE LATTICE AND A DISK-MATRIX COMPOSITE

Numerical examples of calculation of bounds (4) are given for the elasticity problems in Ref. 6, and for the conductivity problems in Ref. 12; the latter reference also gives second-order as well as two-point statistics of both scale-dependent tensors. In order to illustrate the connection to the classical bounding methods in physics of random media, we study two systems here: (i) a random two-phase lattice, and (ii) a composite with disk inclusions. The first problem is

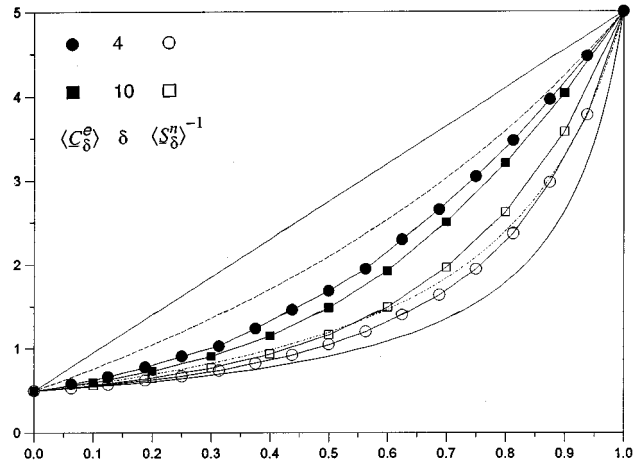

FIG. 2. Bounds on $\mathbf{C}^{\text{eff}}$ of a random two-phase lattice at contrast 10, for all considered volume fractions, showing $\langle C^e_\delta\rangle$ and $\langle S^n_\delta\rangle^{-1}$ at $\delta=4$ and 10; also shown are the Hashin bounds C^H_u and C^H_l.

possibly the simplest setting in which to calculate the hierarchy of bounds for a large range of length scales. It is worthwhile to mention that the random lattice has a continuum counterpart in a random two-phase chessboard, which for a 50% volume fraction of both phases has been solved explicitly in Refs. 13 and 14 with the result

$$C^{\text{eff}}=\sqrt{C_1C_2}. \tag{8}$$

In (8) C_1 and C_2 are the respective conductivities of two phases. Other volume fractions have been studied recently in Ref. 15. The conductivity of a random chessboard is thus a good classical problem on which to test and illustrate our method.

In Figs. 2–4 we show results of $\langle C^e_\delta\rangle$ and $\langle S^n_\delta\rangle^{-1}$ for contrast ratios $C_2/C_1=10$, 10^2, and 10^3, respectively. The window sizes are $\delta=4$ and 10, and an additional $\delta=20$ for the contrast 10^3. For comparison, the classical Voigt, Reuss, and Hashin upper and lower bounds (C^V,C^R,C^H_u, and C^H_1)

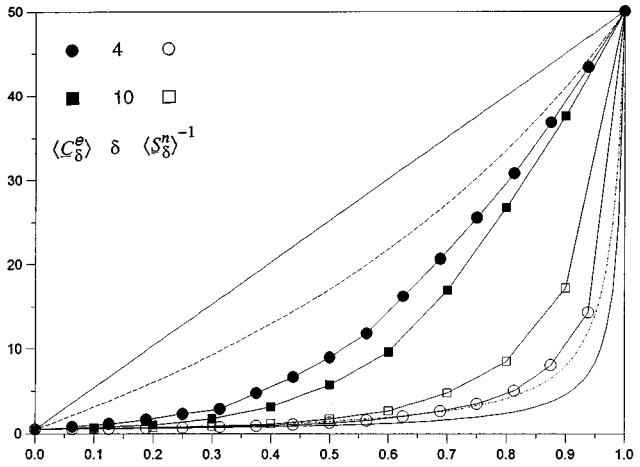

FIG. 3. Bounds on $\mathbf{C}^{\text{eff}}$ of a random two-phase lattice at contrast 100, for all considered volume fractions, showing $\langle C^e_\delta\rangle$ and $\langle S^n_\delta\rangle^{-1}$ at $\delta=4$ and 10; also shown are the Hashin bounds C^H_u and C^H_l.

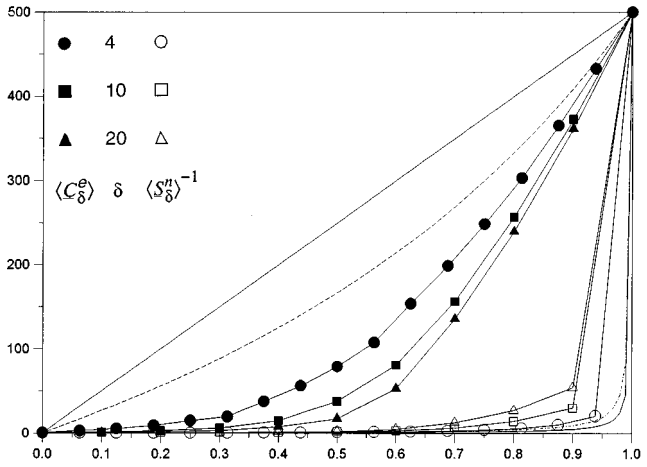

FIG. 4. Bounds on $\mathbf{C}^{\text{eff}}$ of a random two-phase lattice at contrast 1000, for all considered volume fractions, showing $\langle C^e_\delta\rangle$ and $\langle S^n_\delta\rangle^{-1}$ at $\delta=4$, 10, and 20; also shown are the Hashin bounds C^H_u and C^H_l.

are plotted as well. The latter are given by the following well-known equations (see, e.g., Ref. 16)

$$\begin{aligned} C^V&=C_1f_2+C_2f_2,\\ C^R&=[f_1/C_1+f_2/C_2]^{-1},\\ C^H_u&=C_2+f_1[1/[C_1-C_2]+f_2/2C_2]^{-1},\\ C^H_1&=C_1+f_2[1/[C_2-C_1]+f_1/2C_1]^{-1}, \end{aligned} \tag{9}$$

where f_1 and f_2 stand for the volume fraction of either phase. From Figs. 2–4 an improvement in bounds with increasing δ may be observed, which leads, already at $\delta=4$, to estimates comparable, or better, than the Hashin bounds.

All the presented plots were obtained from numerical calculations involving one node of a latter per one board of the chessboard. This is, of course, a crude approximation with respect to the singularity problem at the corners and, therefore, does not represent a piecewise continuum system for which the Hashin bounds and (8) are correct. Consequently, the effective conductivities in our two-phase lattices are lowered, i.e., increasing the number of nodes per board, would lead to an increase of these conductivities, and to a slight asymptotic raising of the $\langle \mathbf{C}^e_\delta\rangle$ and $\langle \mathbf{S}^n_\delta\rangle^{-1}$ values towards those calculated by the continuum theories. It is possible to account for the corner points by using specialized numerical methods, but an adaptation of such a technique to a large domain involving many corners, in order to grasp the scale effects, would be a formidable task. This is a separate issue that we do not pursue here.

Finite-size scaling of $\langle \mathbf{C}^e_\delta\rangle$ and $\langle \mathbf{S}^n_\delta\rangle^{-1}$ is obtained by calculating larger lattices up to $\delta=400$ at volume fraction of 50%. We find the bounds to scale as

$$\langle C^e_\delta\rangle\sim\exp(-\delta^{-p}),\quad \langle S^n_\delta\rangle^{-1}\sim\exp(\delta^{-q}), \tag{10}$$

where p and q are themselves functions of the contrast α. The latter are actually found to be of hyperbolic form

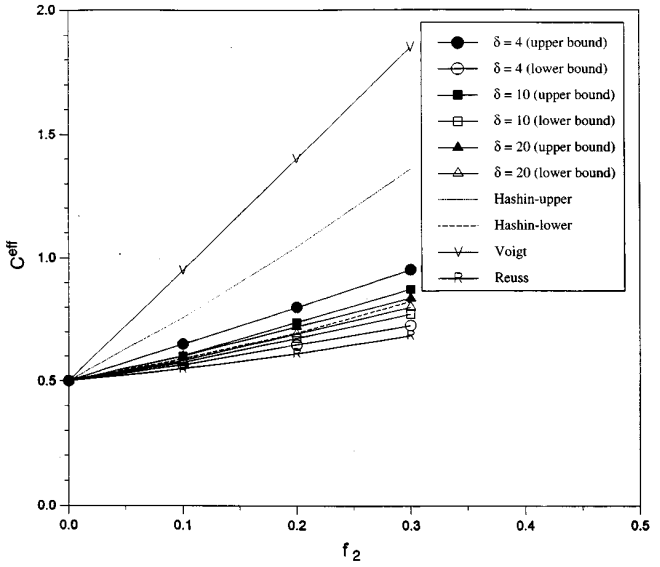

FIG. 5. The scale-dependent upper and lower bounds $\langle C^e_\delta \rangle$ and $\langle S^n_\delta \rangle^{-1}$ on the effective stiffness tensor C^{eff}, plotted vs volume fraction f_2 of inclusions, for windows at $\delta = 4$, 10, 20; the respective Voigt, Reuss, and Hashin bounds are also shown.

$$p(\alpha) = 3.8\alpha^{0.14}, \quad q(\alpha) = 2.4\alpha^{0.59}. \tag{11}$$

Note that the limits of $\alpha \to 1$ and $\alpha \to \infty$ are correctly recovered here. In the first case $\langle \mathbf{C}^e_\delta \rangle \to \langle \mathbf{S}^n_\delta \rangle^{-1} \to C_1 = C_2$, while in the second case C_1 is the limit. Based on some calculations of random disk composites and random polygon mosaics, which we have investigated so far, we conjecture that these are universal relations for finite-size scaling of both bounds in two-phase random systems.

Considering the case $\alpha \to \infty$ leads one to ask about the performance of both bounds at the percolation transition for our ''site problem.'' It is known (e.g., Ref. 16) that the latter occurs at the volume fraction $\sim 59.23\%$, and thus we performed calculations just below, right at, and just above this volume fraction. We have found that both bounds correctly display the percolation transition that is accompanied, as one might expect, by strong fluctuations which decrease with increasing δ. Note that, because we use one lattice node per square, we truly deal with a site problem on a random lattice rather than a continuum problem on a random chessboard.

Turning now to the disk-matrix composite, in Fig. 5 we present a comparison of the δ-dependent bounds (4) with the classical Voigt $\mathbf{C}^V$, Reuss $\mathbf{C}^R$, as well as the upper and lower Hashin bounds $\mathbf{C}^H_u, \mathbf{C}^H_l$. This figure depicts the δ-dependent upper and lower bounds on the effective conductivity tensor of windows $B(\omega)$ for $\delta = 4,10,20$ as a function of the volume fraction of disks when $C_1 = 5.0$ and $C_2 = 0.5$. In order to avoid the problem of narrow necks forming between neighboring inclusions, a minimum spacing of inclusions' centers equal to 1.4 of their diameter has been enforced. With this restriction an upper volume fraction of about 30% can be reached, and thus we terminate all the plots in Fig. 5 at this value. The classical Voigt, Reuss, as well as the upper and lower Hashin bounds calculated according to (9) are also shown. It is well known[17] that the lower (upper) Hashin bound corresponds to a system of disks of higher (lower) conductivity than that of the matrix, and thus the upper and lower bounds converge to the C^H_l bound as δ increases. However, one would need a window of infinite size ($\delta \to \infty$) to actually obtain this homogenization limit.

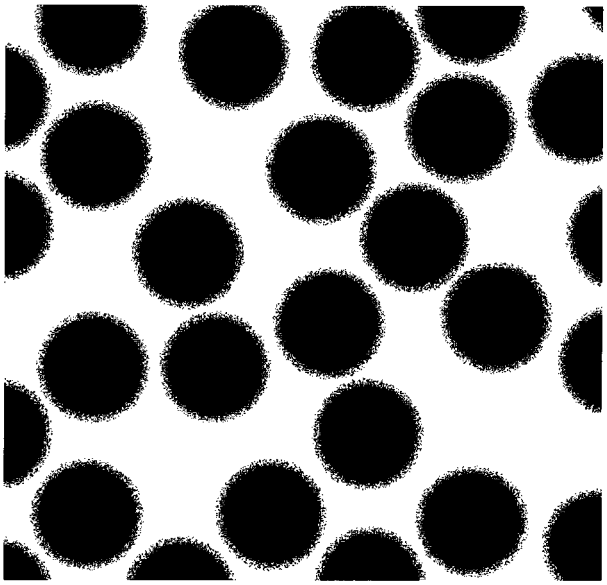

FIG. 6. A matrix-inclusion composite with functionally graded interphases; 47.2% volume fraction of the inclusion (black) phase.

IV. FUNCTIONALLY GRADED COMPOSITES

Interfaces in heterogeneous materials influence their local fields and effective properties.[7,8] Theoretical studies in this area represent the interface as either a well-defined bounding surface between two phases (inclusion disks and matrix), or as a diffuse region of random interpenetration of these two phases having a certain microstructure, which is called an *interphase*.[9] Thus, in the case of a two-dimensional disk-matrix composite, the interface is either a well-defined circle where the properties change discontinuously, or a two-dimensional ring-shaped interphase, see Fig. 6. In this paper we focus on the thermal conductivity of such a system. Note that by virtue of mathematical analogies, the problem is equivalent to the problem of the effective transverse conductivity of a unidirectional composite material, the effective shear modulus of such a material, and several other problems in transport theories. Relevant examples, where the diffuse zone is of a non-negligible size, are interphases in carbon-fiber epoxy composites and in ceramics.

In the following, the disk-matrix interphase is taken as a finite thickness zone of two randomly mixed phases of disk and matrix material. We assume that the matrix (1) and the disk (2) phases are locally homogeneous and isotropic, that is, they are described by two constant isotropic conductivities C_1 and C_2. *Contrast* is defined by C_2/C_1.

In such a composite we find three different length scales: (i) the fine structure of the interphase region, (ii) the size and spacing of functionally graded inclusions, and (iii) the macroscopic dimension of the composite. Spatial randomness on the first two of these precludes any rigorous analytical solution of the problem.

The random mixture of two types of phases (matrix, 1;

disk, 2) in the interphase is represented by a random distribution of two phases which is described by an indicator function:

$$\chi(\vec{r},\omega)=\begin{cases}1 & \text{if } \vec{r}\in V_2,\\ 0 & \text{if } \vec{r}\in V_1,\end{cases} \qquad \vec{r}=(r,\theta), \quad \omega\in\Omega, \tag{12}$$

where V_s is the domain occupied by a phase $s=1$ or 2, respectively; Ω is the sample space, or space of all possible realizations; and ω is one realization of an interphase.

The indicator function χ is characterized in terms of the probability distribution $P\{\chi(r)\}$ where r is the radius of a disk inclusion in its local polar coordinate system. For a functionally graded interphase we assume $P\{\chi(r)\}$ to be axisymmetric and linear,

$$P\{\chi(r)=1\}=Ar+B, \tag{13}$$

where A and B are determined by the conditions

$$P\{\chi(a)=1\}=1 \quad \text{and} \quad P\{\chi(b)=1\}=0, \tag{14}$$

in which a is the disk radius (i.e., the inner radius of the interphase), and b is the outer radius of interphase. Since the disk and the matrix phases are both taken as locally isotropic, Eqs. (12) and (13) are consistent with the statement that the conductivity $\mathbf{C}$ equals $\mathbf{I}C_2$ at $r\leqslant a$, and $\mathbf{I}C_1$ at $r\geqslant b$.

In order to calculate the effective conductivity tensor $\mathbf{C}^{\text{eff}}$ of such a composite, an appropriate computational method is required. To that end we consider a window whose mesh domain is discretized with a 1000×1000 finite difference mesh, where every mesh node represents a micrograin of the composite. In this example the inner and outer radii of inclusions are $a=50$ and $b=60$, respectively, with the inclusions' centers being not closer than 120 units apart; the heterogeneities in the interphase are of size 1 (i.e., the single micrograin size). Thus, a calculation of δ based on the inner (outer) diameter of inclusions gives $\delta=10$ (8.333, respectively), while a calculation based on the size of interphase heterogeneities gives $\delta=1000$. The volume fraction of the inclusion phase (C_2) in Fig. 6 equals 47.2%.

The actual computation of a boundary value problem on a 1000×1000 finite difference mesh involves the solution of a linear algebraic problem with 10^6 degrees of freedom, which is solved by a standard linear algebra package.[18]

In Fig. 7 we present six bounds on the effective conductivity $\mathbf{C}^{\text{eff}}$ of the composite of Fig. 1 for a range of contrast from 1 through 10^4. As expected, the Voigt and Reuss bounds become very wide with the increasing contrast, and the Hashin bounds perform only slightly better. On the other hand, the bounds obtained from the essential and natural boundary conditions are very close, even at contrast 10^4, as compared to the performance of the Hashin bounds. This is especially remarkable in view of the fact that a window only ten times larger than the disk size has been employed. Interestingly, the use of a window only three times larger would result in bounds very comparable to those of Hashin, indicating how fast the present method converges with an increasing δ.

From the log-log diagram in Fig. 7 it can be seen that $\mathbf{C}^e=\mathbf{I}C^e$ shows a scaling with the contrast, i.e., $C^e=(C_2/C_1)^{0.7}$. On the other hand, $\mathbf{C}^n=\mathbf{I}C^n$ scales with nearly the same exponent up to 10^3, and for higher contrasts a different dependency is observed.

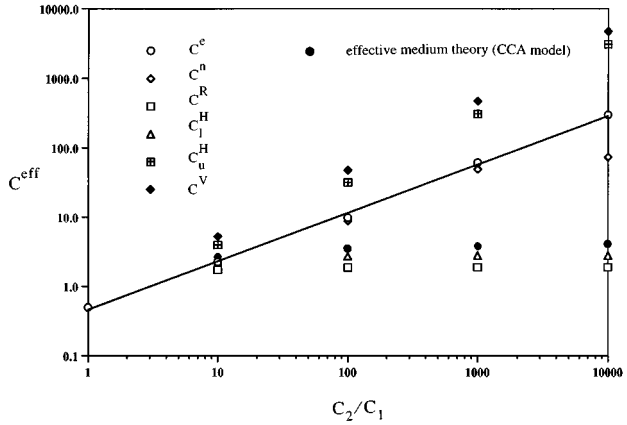

FIG. 7. C^{eff} of a composite with graded interphases such as shown in Fig. 6. Shown are the Voigt, Reuss, Hashin upper and lower bounds, and C^e_δ and $C^n_\delta\equiv(S^n_\delta)^{-1}$ at $\delta=10$ with respect to the inner disk diameter, as well as the results of the effective-medium theory (CCA model)—all as a function of contrast.

Another major conclusion concerns the effect of the presence of an interphase on $\mathbf{C}^{\text{eff}}$ of a functionally graded composite as compared to the case of perfect inclusions. Note that the case of perfect disks falls exactly on the lower Hashin bound. Thus, we see that small fuzziness, i.e., a fuzzy inclusion with a ring of thickness 20% of the disk radius a dramatically increases $\mathbf{C}^{\text{eff}}$ as compared to the perfect disks case. The reason for this is that fuzzy zones tend to interconnect the inclusion phase through the composite, although no percolation takes place at the volume fractions studied here.

V. EFFECTIVE-MEDIUM THEORY FOR A FUNCTIONALLY GRADED COMPOSITE

A natural way to establish an effective medium theory for a graded composite is to use the composite cylinder assemblage (CCA) model of Hashin and Rosen.[19,20] In this model the unidirectional composite is represented as a set of composite cylinders which completely fill the space. Each composite cylinder consists of a cylindrical fiber (i.e., a disk in the transverse conductivity problem) enclosed in two concentric cylinders, the inner one representing the interphase and the outer one the matrix. Furthermore, each composite cylinder has a similar geometry such that a/b and a/c are constant, where a, b, and c are the radius of the fiber, the outside radius of the interphase, and the outside radius of the matrix (and the composite cylinder), respectively.[21]

When calculating the effective conductivity of the composite we can apply, in principle, either essential or natural boundary conditions, but for the composite cylinder assemblage model both will yield identical results. In this presentation we choose to apply a uniform temperature gradient field $\overline{\nabla T}=(\overline{T}_{,1},0)$ such that on the boundary of the composite we have

$$T|_{r=c}=\overline{T}_{,1}c\cos\theta. \tag{15}$$

The governing equation for our problem is the heat equation which for case of no coupling between mechanical and thermal fields and steady-state condition is

$$-\mathrm{div}\vec{q}=C^{(s)}\Delta T=0, \quad s=d,m \tag{16}$$

for two homogeneous and isotropic regions of disk and matrix, and

$$-\mathrm{div}\vec{q}=\nabla(\mathbf{C}^{(i)}\cdot\nabla T)=0 \tag{17}$$

in the inhomogeneous interphase. While the properties of fiber and matrix are constant, those of the interphase are assumed to be of the form

$$C^{(i)}=Ar^{Q}, \tag{18}$$

where A and Q are found from two end conditions: $C^{(i)}=C^{(d)}$ and $C^{(m)}$ at $r=a$ and $r=b$, respectively. The distribution (18) is the only type of a function that allows a closed-form solution of the set of governing equations, see Eq. (22) below. It has been found to very well approximate the actual graded microstructure of the interphase.[9]

Equation (16) is the Laplace's equation which yields the temperature fields in the fiber as

$$T^{(d)}=A^{(d)}r\cos\theta, \quad 0\leqslant r\leqslant a, \tag{19}$$

and in the matrix as

$$T^{(m)}=[A^{(m)}r+B^{(m)}/r]\cos\theta, \quad b\leqslant r\leqslant c. \tag{20}$$

Equation (17) for the interphase region takes the following form in polar coordinates:

$$C^{(i)}\frac{\partial^2 T}{\partial r^2}+\left[\frac{\partial C^{(i)}}{\partial r}+\frac{1}{r}C^{(i)}\right]\frac{\partial T}{\partial r}+\frac{C^{(i)}}{r^2}\frac{\partial^2 T}{\partial\theta^2}=0. \tag{21}$$

The general solution is

$$T=(A^{(i)}r^{\lambda_1}+B^{(i)}r^{\lambda_2})\cos\theta, \quad a\leqslant r\leqslant b. \tag{22}$$

Finally, we evaluate the five unknown constants $A^{(d)}$, $A^{(i)}$, $B^{(i)}$, $A^{(m)}$, $B^{(m)}$ by using the boundary conditions

$$\left.\begin{aligned}T^{(d)}&=T^{(i)}\\ q^{(d)}&=q^{(i)}\end{aligned}\right\} \quad \text{at } r=a, \tag{23}$$

$$\left.\begin{aligned}T^{(i)}&=T^{(m)}\\ q^{(i)}&=q^{(m)}\end{aligned}\right\} \quad \text{at } r=b, \tag{24}$$

$$T^{(m)}=\overline{\nabla T}c\cos\theta \quad \text{at } r=c \tag{25}$$

with

$$q^{(s)}=-C^{(s)}\frac{\partial T^{(s)}}{\partial r}, \quad s=d,i,m. \tag{26}$$

This permits to calculate the effective conductivity $\mathbf{C}^{\mathrm{eff}}$ by equating the flux on the boundary of our composite cylinder $q^{(m)}(c)$ with the flux in the equivalent homogeneous cylinder having the effective properties

$$q^{(m)}(c)=-C^{\mathrm{eff}}\overline{\nabla T}\cos\theta, \tag{27}$$

which yields

$$\mathbf{C}^{\mathrm{eff}}=\mathbf{I}C^{\mathrm{eff}}, \quad C^{\mathrm{eff}}=\frac{C^{(m)}}{\overline{\nabla T}}\left(A^{(m)}-\frac{B^{(m)}}{c^2}\right). \tag{28}$$

It is found that the above model predicts effective-medium properties well for low contrasts only; this is investigated in detail in Ref. 22. For C_2/C_1 greater than 10, $\mathbf{C}^{\mathrm{eff}}$ tends to be underestimated as is shown in Fig. 7. The reason for this lies in the inability of the composite cylinder model to grasp the connectivity effects between all the disks with graded interphases in the composite medium, that lead to a dramatic change in $\mathbf{C}^{\mathrm{eff}}$ with respect to the perfect disk composite.

Four other effective-medium methods could be developed for this type of a composite with functionally graded interphases: (a) a generalized self-consistent method (three phase model) (see references in Ref. 20), (b) a Mori-Tanaka model (see references in Refs. 4 and 20), (c) a differential scheme,[23] (d) a self-consistent model (see references in Refs. 4 and 20). Methods (a) and (b) would result in the same solution as the CCA. On the other hand, (c) and (d) would result in coupled differential equations requiring a quite extensive analysis. Also, such methods are known to be questionable and possibly invalid at high contrasts.

VI. CONCLUSIONS

We have shown that the method of essential and natural boundary conditions leads to a very practical procedure of bounding the effective conductivity of random-heterogeneous media. For any choice of a length scale two boundary value problems need to be solved that always result in rigorous bounds on $\mathbf{C}^{\mathrm{eff}}$. The resulting hierarchy of bounds shows that with the increasing length scale ever more accurate bounds can be achieved. The method may be used on small length scales without a need of solving large lattices as is done in case of the periodic boundary conditions.

The rapid convergence of both bounds with increasing δ has been illustrated on two simple examples: that of a disk-matrix composite for which $\mathbf{C}^{\mathrm{eff}}$ is know to be given by the lower Hashin bounds, and that of a random two-phase lattice. The latter case served to derive finite-size scaling formulas for both bounds. The formulas are proposed to have a wider, more universal, applicability than just for random lattices.

The rapid convergence of both bounds is especially useful in the problem of a composite with graded interphases. It is observed that boundary value problems on the length scale of just ten times the size of inclusions can be bounded even at very high contrasts, up to 10^3 and 10^4. Furthermore, we determined that the presence of a narrow graded interphase has a dramatic effect on $\mathbf{C}^{\mathrm{eff}}$ as compared to the case of perfect disks. In fact, $\mathbf{C}^{\mathrm{eff}}$ is found to scale as $(C_2/C_1)^{0.7}$ over contrasts ranging from 1 through 10^3.

The approach developed in this paper represents new treatments of (i) transport problems and (ii) functionally graded materials. In general, a more complete study of (ii) is required that will consider a larger parameter space, include different types of spatial inhomogeneity, and explore the effects of other material geometries. Finally, it should be noted that the same method can be applied to transport and elasticity problems of a number of other types of multiscale microstructures.

ACKNOWLEDGMENTS

We benefited from many discussions and interaction with I. Jasiuk of Michigan State University. The authors are grateful to the reviewers for comments and suggestions. This research was funded in part by NSF Grant No. MSS-9202772 and the Research for Excellence Fund from the State of Michigan. Support by the Computer Science Departments at Texas A&M University and the Sandia National Laboratory is gratefully acknowledged.

APPENDIX

For the completeness of the paper we sketch here a proof of the hierarchies (4) of bounds on $\mathbf{C}^{\text{eff}}$. Let us introduce a partition of a square-shaped window $B_\delta(\omega)$, of volume V_δ, into four smaller square-shaped windows $B^s_{\delta'}(\omega), s=1,\ldots,4$, of size $\delta'=\delta/2$ and volume $V_{\delta'}$ each. Also, let us introduce a restricted version of the essential boundary condition (2), i.e.,

$$T^r=\overline{\nabla T}\cdot x. \tag{A1}$$

Condition (A1) is more restricting then the original (2) in the sense that (A1) applies to the boundaries of all $B^S_{\delta'}(\omega)$ rather than just $B_\delta(\omega)$; the superscript ''r'' indicates a restriction. Now, observe that a variational principle[1,3] implies that the rate of irreversible entropy production $\Phi^r(\omega)$ stored in the body

$$B_\delta(\omega)=\bigcup_{s=1}^{4} B^s_{\delta'}(\omega)$$

under the essential boundary condition (A1) bounds the entropy rate $\Phi(\omega)$ stored in the same body under (2)

$$\frac{1}{2}V_\delta\overline{\nabla T}\cdot C^e_\delta\cdot\overline{\nabla T}=\Phi(\omega)\leqslant\Phi^r(\omega)$$

$$=\sum_{s=1}^{4}\frac{1}{2}V_{\delta'}\overline{\nabla T}\cdot C^{e,s}_{\delta'}\cdot\overline{\nabla T}. \tag{A2}$$

Here C^e_δ and $C^{e,s}_{\delta'}$ are the effective conductivity tensors of $B_\delta(\omega)$ and $B^s_{\delta'}(\omega)$, respectively. Upon carrying out ensemble averaging and noting spatial homogeneity and ergodicity of $\boldsymbol{B}$, we obtain from (A2)

$$\langle C^e_\delta\rangle\leqslant\langle C^e_{\delta'}\rangle. \tag{A3}$$

In this way, a sequence of upper δ-dependent bounds is obtained on $C^{\text{eff}}=C^e_\infty$.

Just like we introduced a restricted version of the essential boundary conditions, we can also introduce such a version of the natural boundary condition (3), that is

$$\overline{\vec{q}}\cdot\vec{n}=\vec{q}\cdot\vec{n}, \tag{A4}$$

which applies to the boundaries of all four $B^s_{\delta'}(\omega)$. Next, it follows from the dual variational principle, that the complementary entropy production rate $\Phi^{*r}(\omega)$, as a function of the heat flux, stored in the body

$$B_\delta(\omega)=\bigcup_{s=1}^{4} B^s_{\delta'}(\omega)$$

under condition (A4) bounds the entropy rate $\Phi^*(\omega)$ stored in the same body under (3):

$$\frac{1}{2}V_\delta\overline{\vec{q}}\cdot S^n_\delta\cdot\overline{\vec{q}}=\Phi^*(\omega)\leqslant\Phi^{*r}(\omega)$$

$$=\sum_{s=1}^{4}\frac{1}{2}V_{\delta'}\overline{\vec{q}}\cdot S^{n,s}_{\delta'}\cdot\overline{\vec{q}}. \tag{A5}$$

Here S^n_δ and $S^{n,s}_{\delta'}$ are the effective resistivity tensors of $B_\delta(\omega)$ and $B^s_{\delta'}(\omega)$, respectively. Upon carrying out ensemble averaging and noting spatial homogeneity and ergodicity of $\boldsymbol{B}$, we obtain from (A5)

$$\langle S^n_\delta\rangle\leqslant\langle S^n_{\delta'}\rangle. \tag{A6}$$

The sequence of lower δ-dependent bounds on $\mathbf{C}^{\text{eff}}$ is obtained by simply inverting (A6). Combining this with (A3), we obtain the hierarchy (4).

[1] M. J. Beran, *Statistical Continuum Theories* (Wiley-Interscience, New York, 1968); J. R. Willis, Adv. Appl. Mech. **21**, 1 (1981).

[2] R. Burridge, S. Childress, and G. Papanicolau, *Macroscopic Properties of Disordered Media* (Springer-Verlag, Berlin, 1982).

[3] S. Torquato, Appl. Mech. Rev. **44**, 37 (1991).

[4] S. Nemat-Nasser, and M. Hori, *Micromechanics: Overall Properties of Heterogeneous Solids* (North-Holland, Amsterdam, 1993).

[5] C. Huet, J. Mech. Phys. Solids **38**, 813 (1990); K. Sab, Eur. J. Mech. A/Solids **11**, 585 (1992).

[6] C. Huet, in *Continuum Models and Discrete Systems 2*, edited by G. A. Maugin (Longman Scientific & Technical, New York, 1991), p. 127; C. Huet, in *PROBAMAT-Probabilities and Materials: Tests Models and Applications*, Vol. 269 of *NATO Advanced Research Workshop, Series E* (Kluwer, Dordrecht, 1994), p. 241.

[7] J. D. H. Hughes, Comp. Sci. Technol. **41**, 13 (1991).

[8] R. J. Kerans *et al.*, Ceram. Bull. **68**, 429 (1989).

[9] I. Jasiuk and M. Ostoja-Starzewski, in *Control of Interfaces in Metal and Ceramics Composites*, edited by R. Y. Lin and S. G. Fishman (Minerals, Metals & Materials Society, Pennsylvania, 1994), p. 317.

[10] M. Ostoja-Starzewski, I. Jasiuk, W. Wang, and J. Schulte, in *Proceedings of the 3rd International Symposium on Structural and Functional Gradient Materials*, edited by B. Ilschner and N. Cherradi (Presses Polytechniques et Universitaires Romandes, Switzerland, 1995), p. 259.

[11] M. Ostoja-Starzewski, Prob. Eng. Mech. **8**, 107 (1993).

[12] M. Ostoja-Starzewski, Appl. Mech. Rev. **47**, S221 (1994).

[13] J. B. Keller, J. Math. Phys. **5**, 548 (1964).
[14] A. M. Dykne, Sov. Phys. JETP **7**, 548 (1970).
[15] L. Berlyand, Phys. Rev. B **50**, 4 (1994).
[16] R. Durret, *Lecture Notes on Particle Systems and Percolation* (Wadsworth and Brooks, Pacific Grove, 1988).
[17] Z. Hashin, J. Appl. Mech. **50**, 48 (1983).
[18] SLAPACK, Lawrence Livermore National Laboratory.
[19] Z. Hashin and B. W. Rosen, J. Appl. Mech. **31**, 223 (1964).
[20] R. M. Christensen, *Mechanics of Composite Materials* (Wiley, New York, 1979).
[21] I. Jasiuk and M. W. Kouider, Mech. Mater. **15**, 53 (1993).
[22] M. Ostoja-Starzewski, I. Jasiuk, W. Wang, and K. Alzebdeh, Acta Mater. **44**, 2057 (1996).
[23] A. N. Norris, Mech. Mater. **4**, 1 (1985).